

Unfolding kinetics of periodic DNA hairpins

Sandra Nostheide^a, Viktor Holubec^b, Petr Chvosta^b and Philipp Maass^a

^a Fachbereich Physik, Universität Osnabrück, BarbarasträÙe 7, 49076 Osnabrück, Germany

^b Department of Macromolecular Physics, Faculty of Mathematics and Physics, Charles University, CZ-180 00 Praha, Czech Republic

E-mail: chvosta@kmf.troja.mff.cuni.cz, philipp.maass@uni-osnabrueck.de

Abstract. DNA hairpin molecules with periodic base sequences can be expected to exhibit a regular coarse-grained free energy landscape (FEL) as function of the number of open base pairs and applied mechanical force. Using a commonly employed model, we first analyse for which types of sequences a particularly simple landscape structure is predicted, where forward and backward energy barriers between partly unfolded states are decreasing linearly with force. Stochastic unfolding trajectories for such molecules with simple FEL are subsequently generated by kinetic Monte Carlo simulations. Introducing probabilities that can be sampled from these trajectories, it is shown how the parameters characterising the FEL can be estimated. Already 300 trajectories, as typically generated in experiments, provide faithful results for the FEL parameters.

PACS numbers: 05.70.Ln, 02.50.-r, 05.10.Gg

1. Introduction

Single-molecule experiments deliver previously unprecedented insights into kinetics and thermodynamics of biophysical and biochemical processes [1, 2, 3]. One class of these experiments comprises unfolding and folding of DNA (or other biomolecules) under application of mechanical forces by optical or magnetic tweezers, or an atomic force microscope [4, 5, 6, 7, 8, 9, 10, 11, 12, 13, 14, 15, 16]. An important aim of these studies is to obtain information on free energy differences (FEDs) between folded and unfolded states, or, more generally, on the free energy landscape (FEL) characterising both the levels of stable as well as metastable, partly unfolded states and the energy barriers in between them.

Equilibrium methods are the easiest way to determine FEDs. In these the Boltzmann statistics is applied to the fraction of residence times of the states at different values of the control parameters [5, 9, 10, 17, 18, 19]. However, for many molecules the barriers between states turn out to be so large that an equilibrium is not achieved within the available experimental time window [5, 18, 20].

An intriguing way to measure FEDs from out-of-equilibrium measurements is made possible by utilising detailed and integral work fluctuation theorems [21, 22], as the Crooks fluctuation theorem [23], or its integral counterpart, the Jarzynski equality [24]. Analogous to the Boltzmann distribution in equilibrium, these theorems hold true in an universal way independent of microscopic details of the molecule and its unfolding/folding dynamics. Work in the fluctuation theorems refers to the thermodynamic work under a certain driving protocol $\lambda(t)$ of control variables during a time interval $[t_i, t_f]$, as, for example, pulling a molecule with a force $f(t)$. Because of the strong fluctuations in single molecule experiments, work values W become stochastic variables with a distribution $p(W)$.

The Crooks theorem states that work distributions $p(W)$ and $p_R(W)$ for a protocol $\lambda(t)$ and the associated reversed protocol $\lambda_R(t) = \lambda(t_i + t_f - t)$, respectively, are related according to $p(W)/p_R(-W) = e^{(W-\Delta F)/k_B T}$ [23], where $\Delta F = F_f - F_i$ is the difference in (equilibrium) free energies $F_{i,f}$ of the molecule in the macrostates specified by the control variables $\lambda_{i,f} = \lambda(t_{i,f})$, and $k_B T$ is the thermal energy. In cases where the Crooks theorem [23] can not be used, e. g., because the work for the reverse process can not be obtained with sufficient statistics [12, 25, 26], the Jarzynski equality offers an alternative way to the FED. This theorem states that $\langle e^{-W/k_B T} \rangle = \int dW p(W) e^{-W/k_B T} = e^{-\Delta F/k_B T}$ [24] and has been applied successfully in various cases [13, 26, 27, 28]. In general, however, the application of the Jarzynski equality turns out to be difficult, because $\langle e^{-W/k_B T} \rangle$ is dominated by rare trajectories with work values $W < \Delta F$ [24, 28, 29, 30]. A possible solution is to extend measured histograms of (typical) work values to the tail regime $W \ll \Delta F$ by fitting to theoretical predictions. To this end, some generic behaviour in the tail regime needs to be assumed and attempts have been made recently in this direction [31, 32, 33]. Even under some assumption of the functional form of the tail, the extraction of reliable free energy estimates from the measured data requires care, because one needs to correctly take into account the dependence of biasing effects on the number of measurements (single unfolding trajectories) [28, 29, 30, 33, 34, 35, 36, 37].

If the statistics is not sufficient to allow reasonable application of the nonequilibrium fluctuation theorems, an alternative route for determining the FED, and more generally, the FEL, is to analyse the kinetics of unfolding and/or folding, and to compare it with predictions from theories. This requires to introduce parameters that are specific for the molecule under investigation. For example, it was shown [9] that one can extract the FEL out of first rupture force distributions. By considering a two-state DNA folder these distributions for both the unfolding and folding process are connected to the distributions of the survival probabilities in the folded and unfolded state. In the case of constant loading/unloading rates, a clever representation [9] of the survival probabilities allows one to determine energetic barriers and the FED between the two states.

It is clear that such methods heavily rely on a good theoretical description of the kinetics of DNA unfolding and folding. These are commonly based on coarse-grained approaches, where molecular states are specified by the number n of open base pairs (bps). Models have been established in the past [8, 20, 38, 39, 40, 41, 42, 43] that

faithfully describe the free energies of these states and their variation with an externally applied force f in terms of a FEL $G(n, f)$. An important task is to optimise parameters in such models by suitable measurements, and to determine their variation under change of the environment, such as salt concentration, pH value or temperature of the solvent.

So far analytical treatments concentrated on two-state folders. In experiments often long sequences are considered which exhibit many minima in the FEL associated with partly unfolded states. An advantage of these sequences is that one unfolding/folding process involves many transitions, each of them giving information on the FEL. On the other hand, theoretical treatments of the unfolding and folding kinetics of multistate folders are difficult because each transition between successive minima is characterised by distinct barriers and energy differences between the involved states. It is thus useful to consider periodic DNA sequences where transitions between states are characterised by the same energetic parameters. In this work we will model the unfolding kinetics of such periodic DNA sequences and investigate whether it is possible to obtain reliable information on the FEL based on a small number of unfolding trajectories. Using standard modelling, we first show that simple regular FELs can be obtained for periodic sequences, which keep their characteristics over a wide range of pulling forces. KMC simulations are then applied to generate unfolding trajectories for these sequences, as surrogate for experimental ones. By fitting survival and persistence probabilities obtained from these trajectories to analytical results, we demonstrate that already about 300 trajectories can give good estimates of FEL parameters.

2. Free energy landscapes (FELs)

In a coarse-grained approach, unfolding of DNA (and other molecules) is often described by thermally activated transitions between minima of a FEL $G(n, f)$, which is expressed as a function of the number n of sequentially opened bps and the applied stretching force f . It can be decomposed as [9, 12, 38]

$$G(n, f) = G_{\text{form}}(n) + G_{\text{str}}^{\text{ss}}(n, f) - f\Delta x_l^{\text{ss}}, \quad (1)$$

where the force-independent "formation" part $G_{\text{form}}(n)$ quantifies the free energy release upon breaking of n bps, and the part $-f\Delta x^{\text{ss}}$ describes the energetic preference of unfolded states for larger f ; Δx^{ss} is the length of the unfolded single-stranded (ss) part. The force-dependent "stretching" part $G_{\text{str}}^{\text{ss}}(n, f)$ takes into account the decrease of entropy of the ssDNA when increasing the end-to-end distances of the unfolded parts [9]. Models borrowed from polymer physics are commonly used to specify $G_{\text{str}}^{\text{ss}}(n, f)$. For the most prominent examples, the freely jointed chain (FJC) [44] and the worm-like chain (WLC) model [45], we give details in Appendix A.

For $G_{\text{form}}(n)$ we use the nearest neighbour (NN) model [46, 47]

$$G_{\text{form}}(n) = \sum_{\mu=n+1}^{n_{\text{tot}}-1} \epsilon_{\mu, \mu+1} + G_{\text{loop}}(1 - \delta(n, n_{\text{tot}})), \quad (2)$$

where $\epsilon_{\mu,\mu+1}$ is the interaction energy between adjacent bases (see Appendix A for an example). This model has been applied successfully in various experiments [8, 9, 20, 38, 42, 43, 48, 49], and its parameters have been continuously improved. We take the ones recently reported in [11] with the parameter values listed in the table A1 in Appendix A.

At zero force, the free energy $G(n, f = 0) = G_{\text{form}}(n)$ of long unbranched hairpin molecules without any additional structures such as, e. g., interior loops, increases monotonically with n , with varying local rise $\Delta G_{\text{form}}(n) = G_{\text{form}}(n + 1) - G_{\text{form}}(n)$. Considering unzipping experiments with a constant loading rate r , corresponding to a force increasing linearly with time,

$$f(t) = f_0 + rt, \quad (3)$$

the FEL gets tilted and local minima ("states") develop at values of n , where $\Delta G_{\text{form}}(n)$ changes significantly, i. e. where $\Delta G_{\text{form}}(n - 1)$ and $\Delta G_{\text{form}}(n)$ differ strongly. Once the tilting is large enough that the level of these minima becomes comparable to the energy of the completely folded state, thermally activated transitions from one minimum to the next drive the molecule into the unfolded state. In general, each of these transitions is characterised by distinct forward and backward barriers, which also evolve differently in time. This implies that theoretical treatments become increasingly difficult with larger number of states.

With the goal to make a theoretical treatment of the kinetics tractable, we are looking for periodic sequences, where the forward and backward barriers decrease linearly with force and where the levels of the states decrease linearly with $f n_\alpha$. Here n_α denotes the particular n values of the states α . To be specific, we write for the forward barriers $\Delta(f)$, the backward barriers $\Delta'(f)$, and the state free energies $G_\alpha(f) \equiv G_{n_\alpha}(f)$:

$$\Delta(f) = \Delta_0 - \Delta_1 f, \quad (4a)$$

$$\Delta'(f) = \Delta'_0 - \Delta'_1 f, \quad (4b)$$

$$G_\alpha(f) = \alpha(g_0 - g_1 f). \quad (4c)$$

Because $G_{\alpha+1}(f) - G_\alpha(f) = \Delta(f) - \Delta'(f)$, it holds $g_0 = \Delta_0 - \Delta'_0$ and $g_1 = \Delta_1 - \Delta'_1$, that means the landscape is specified by four independent parameters. It is sufficient that equations (4a)-(4c) are obeyed in the range where the energy levels start to become comparable to the one of the folded state, that means when for the first time transitions can take place. Whether, on the basis of equation (1), periodic DNA sequences satisfying equations (4a)-(4c) can be found will be discussed in the next section.

3. Landscapes of periodic DNA sequences

We first analyse unbranched DNA hairpin molecules that have periodic bp sequences without interior loops. For these molecules, equations (4a)-(4c) can be fulfilled over a sufficiently wide force range if the periodicity length L of the units is small enough. It turns out that the minima are not very pronounced and the barriers are just a few

multiples of the thermal energy $k_B T$. Accordingly, FEDs of these sequences should be measurable also from equilibrium occupancy statistics [5, 9, 10, 17, 18, 19]. When considering interior loops attached to the basic units, the requirements imposed by equations (4a)-(4c) can be well fulfilled with typically high barriers between the minima. Additional parameters specifying the change of the FEL by the interior loops [39, 50] then enter the description. We notice that they are less accurate than those defining the bp interactions [11] (see the table A1 in app. Appendix A).

3.1. Hairpin molecules without interior loops

A double-stranded (ds) DNA with periodicity length $L = 5$ bps and an arbitrarily chosen sequence in the period is sketched in figure 1. Such hairpin molecules can, in principle, be branched or form other structural elements. To exclude such features we rely on folding predictions of the program Mfold [39, 50]. FELs for unbranched hairpin molecules, calculated according to equations (1) and (2), in general do not satisfy the requirements in equations (4a)-(4c). Starting from the folded state, minima and barriers first form regularly in the landscape when f is increased up to a certain value. However, by further increasing f , in between them new minima and barriers can form. This means that the overall structure of the regular landscape is not stable, but one regular type goes over to another one. The "new barrier effect" leads to force intervals where equations (4a)-(4c) are satisfied, but jumps of $\Delta(f)$, $\Delta'(f)$ and $G_\alpha(f)$ appear when going from one interval to the next one. Another possibility that the regular structure gets modified is that the positions of minima and saddle points are shifting. This "shifting effect" leads to force intervals where equations (4a)-(4c) are satisfied, but jumps in the slopes Δ_1 , Δ'_1 and g_1 appear when going from one interval to the next. For long periodicity lengths, the new barrier effect is difficult to avoid, even for sequences that are specifically optimised in order to circumvent the problem. On the other hand, for sufficiently short periodicity lengths ($L \lesssim 7$), the new barrier effect is usually not occurring. The shifting effect, however, affects the regular behaviour also for small periodicity lengths. To avoid it, sequences have to be optimised.

An optimisation among all 4^5 sequences for $L = 5$ bps with respect to equations (4a)-(4c) gives the smallest regression coefficients for the sequence consisting of TGCAA [see figure 2(b)], which we refer to as sequence I. The intercept and slope parameters of the linear functions for this sequence I are given in the table 1. The

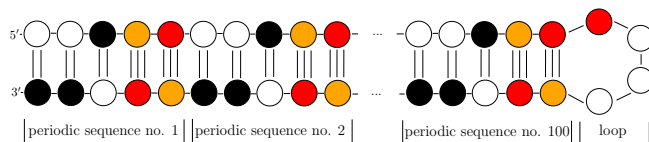


Figure 1. Sketch of a periodic, random DNA hairpin structure with a periodicity length of $L = 5$ bps. The bases are coloured as follows: adenine (white), cytosine (orange), guanine (red) and thymine (black).

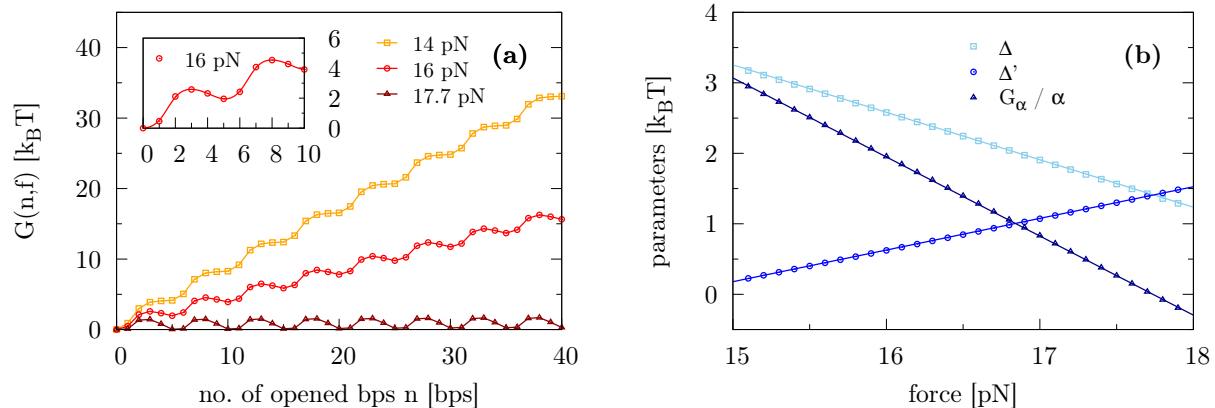


Figure 2. (a) FEL for the periodically continued sequence I for three magnitudes of force. The sequence has TGCAA as basic unit and no interior loops. The inset shows a zoom of the first two barriers for 16 pN. (b) Forward barriers Δ , backward barriers Δ' , and (order-normalised) state energies G_α/α as a function of force for the sequence I. The regression lines show the linear behaviour according to equations (4a)-(4c).

corresponding FEL is depicted in figure 2(a) for three force values $f = 14$ pN (minima have not yet formed), $f = 16$ pN (minima have formed, levels increase with n), and $f = 17.7$ pN (equal level of the minima). The inset shows two barriers zoomed out from the FEL for $f = 16$ pN. Because these barriers are merely $2.8 k_B T$ high, they can be easily surmounted at room temperature and equilibrium methods should be applicable.

3.2. Hairpin molecules with interior loops

For longer basic units, equations (4a)-(4c) can be satisfied by attaching interior loops to each unit. In this case even equal type of bases in the ds parts, e. g. AAA... paired with TTT..., yield local minima in the FEL. This is because the ssDNA in the interior loops has more flexibility, which leads to an entropy rise and accordingly a drop in $G(n, f)$ associated with additional G_{loop} terms in equation (2). Such sequences with equal type

Table 1. Energetic parameters in equations (4a)-(4c) for the three sequences I-III. (I: Optimised sequence with TGCAA as basic unit, without interior loops; II: Basic units with 10 A bases paired with T, separated by interior loops; III: Basic units with mixed types of bases of 16 bps length, separated by interior loops.

parameter	unit	sequence I	sequence II	sequence III
Δ_0	$k_B T$	13.35	26.61	41.53
Δ_1	$\frac{k_B T}{\text{pN}}$	0.67	1.78	1.97
Δ'_0	$k_B T$	-6.55	-0.13	-20.91
Δ'_1	$\frac{k_B T}{\text{pN}}$	-0.45	-0.79	-2.27
g_0	$k_B T$	19.90	26.74	62.45
g_1	$\frac{k_B T}{\text{pN}}$	1.12	2.57	4.23

of bases in the ds parts could be particularly useful to determine improved G_{loop} values in single-molecule experiments.

Let us consider a ds part consisting of bases A and complementary bases T, and an interior loop with TTT attached to the A bases and CCC attached to the T bases. Care was taken that Mfold [39, 50] predicts a linear folding structure for the molecule. The corresponding loop contribution to the free energy G_{loop} is 3.24 kJ/mol. Barrier heights can be regulated by varying the length of the ds part. For example, for 10 bps in the ds part, we find a barrier height of $8.1 k_B T$ at $f = 10.4$ pN, where all minima are at equal level. For a sequence with 20 bps the corresponding force is $f = 12.4$ pN and the barrier height $9.7 k_B T$. We refer to the sequence with 10 bps as sequence II. Its FEL is shown in figure 3(a) for three force values. Figure 3(b) demonstrates that it follows the linear behaviour according to equations (4a)-(4c). The respective intercept and slope parameters of these functions are given in the table 1.

To give an example for mixed types of bases in the ds part, we take one of the branches of the triple-branch molecule investigated earlier in [12, 18] and attach to it the same loop as for the molecule considered above with equal type of bases. Only the order is reversed, that means the CCC bases are located in the strand closer to the 5' end. We refer to this sequence as sequence III. The respective G_{loop} value is 3.23 kJ/mol. Figure 4 depicts the molecule, and its FEL is displayed in figure 5(a) for three force values. As shown in figure 5(b), it follows equations (4a)-(4c). The intercept and slope parameters of the linear functions are listed in the table 1. The barrier height is $12.6 k_B T$ at $f = 14.7$ pN, where all minima are at equal level.

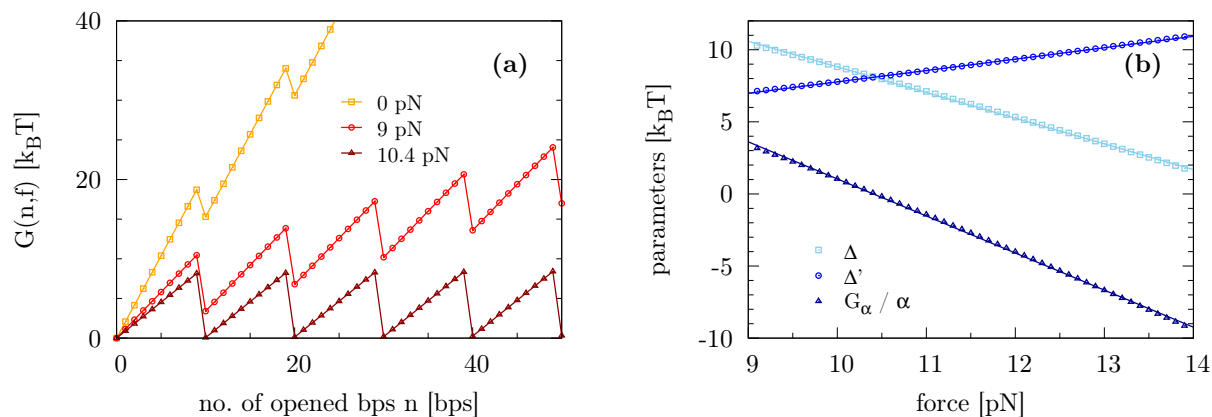


Figure 3. (a) FEL of the sequence II for three magnitudes of force. The sequence is composed of basic units each consisting 10 bases A and complementary bases T, and an interior loop, where TTT is attached to the A bases and CCC to the T bases. (b) Forward barriers Δ , backward barriers Δ' , and (order-normalised) state energies G_α/α as a function of force for the sequence II. The regression lines show the linear behaviour according to equations (4a)-(4c).

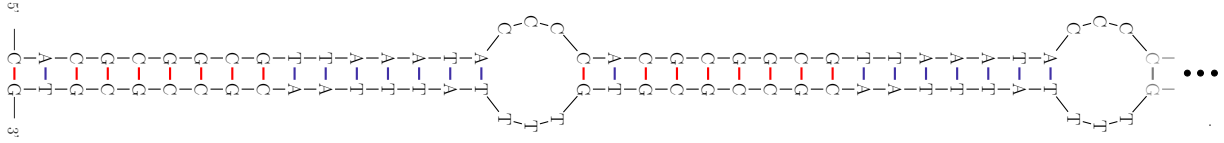


Figure 4. DNA hairpin molecule with sequence III. One basic unit consists of a ds part with mixed types of bases, and a loop of ssDNA attached to it.

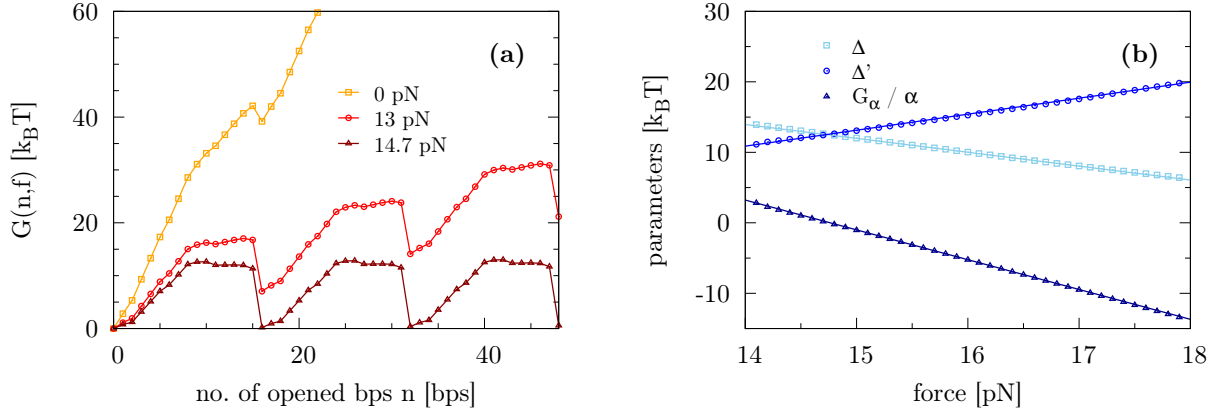


Figure 5. (a) FEL of the sequence III in Fig. 4 for three force values. (b) Forward barriers Δ , backward barriers Δ' , and (order-normalised) state energies G_α/α as a function of force for the sequence III. The regression lines show the linear behaviour according to equations (4a)-(4c).

4. Kinetics and Monte Carlo simulations

According to standard transition rate theory [51], the rate for surmounting the forward barrier is

$$\lambda(f) = \nu \exp[-\beta\Delta(f)], \quad (5)$$

where ν is an attempt frequency and $\beta = 1/k_B T$. A corresponding equation applies to the backward transition rate $\lambda'(f)$ with the backward barrier $\Delta'(f)$ in the exponential. Replacing f by t via equation (3), these rates become

$$\lambda(t) = \nu \exp[-\beta(\Delta_0 - \Delta_1 f_0)] \exp(\beta\Delta_1 r t), \quad (6a)$$

$$\lambda'(t) = \lambda(t) \exp[\beta(g_0 - g_1 f_0)] \exp(-\beta g_1 r t). \quad (6b)$$

For a molecule with m periodic units, the probabilities $p_\alpha(t)$, $\alpha = 0, \dots, m$, of being in state α evolve according to

$$\frac{dp_0(t)}{dt} = -\lambda(t) p_0(t) + \lambda'(t) p_1(t), \quad (7a)$$

$$\frac{dp_\alpha(t)}{dt} = -\lambda(t) [p_\alpha(t) - p_{\alpha-1}(t)] \quad (7b)$$

$$\begin{aligned}
& + \lambda'(t) [p_{\alpha+1}(t) - p_{\alpha}(t)], \quad \alpha = 1, \dots, m-1, \\
\frac{dp_m(t)}{dt} & = \lambda(t) p_{m-1}(t) - \lambda'(t) p_m(t).
\end{aligned} \tag{7c}$$

While for a two-level system ($m = 1$) an explicit solution is given in [52, 53], analytical treatments for larger m become increasingly more difficult. Under neglect of backward transitions, a solution for arbitrary m is given in [54]. Generally, the cumulative rate

$$\begin{aligned}
\Lambda(t, t_0) & = \int_{t_0}^t dt' \lambda(t') \\
& = \frac{\nu \exp[-\beta(\Delta_0 - \Delta_1 f_0)]}{\beta \Delta_1 r} [\exp(\beta \Delta_1 r t) - \exp(\beta \Delta_1 r t_0)]
\end{aligned} \tag{8}$$

enters the solutions [as well as $\Lambda'(t, t_0)$]. With respect to the goal to identify the parameters in equations (4a)-(4c), it is convenient to introduce the probability $\Psi_0(t)$ that, when starting in the folded state ($\alpha = 0$), no transition occurs until time t . This is given by

$$\Psi_0(t) = \exp[-\Lambda(t, 0)]. \tag{9}$$

Because only the forward rate enters this expression, fitting to experimental data should allow one to extract the two parameters Δ_0 and Δ_1 . In order to have access to the two remaining parameters Δ'_0 and Δ'_1 (or g_0 and g_1) in equations (4a)-(4c), we furthermore introduce the probability $\Psi_1(t)$ that, when starting in the folded state ($\alpha = 0$), at least one forward, but no backward transition occurs until time t :

$$\Psi_1(t) = \int_0^t dt_1 \exp[-\Lambda'(t, t_1)] \lambda(t_1) \exp[-\Lambda(t_1, 0)]. \tag{10}$$

The term $\lambda(t_1) \exp[-\Lambda(t_1, 0)]$ is the probability that the first transition occurs at a time t_1 , and the term $\exp[-\Lambda'(t, t_1)]$ is the probability that thereafter no backward transition takes place. For any loading rate, $\Psi_1(t)$ goes through a maximum and approaches a finite value in the long-time limit. Since backward transitions become the less likely the larger r , the maximum can become unnoticeable at high loading rates.

In order to test the procedure, we perform Monte Carlo simulations of the stochastic process with the parameter values listed in the table 1, which we will henceforth refer to as the ‘‘true values’’. In all cases we consider molecules with $m = 4$ periodic units. The probabilities $\Psi_0(t)$ and $\Psi_1(t)$ are sampled from a set of N unfolding trajectories. The simulations can be performed in an efficient manner by using the First Reaction Time Algorithm (FRTA) [55, 56]. Starting from a antecedent transition at time t_0 , one generates a random attempt time t for a successive transition from a uniformly distributed number η in the unit interval by

$$\Lambda(t, t_0) = -\ln(1 - \eta), \tag{11}$$

which yields

$$t = \frac{1}{\beta \Delta_1 \eta} \ln \left(\exp(\beta \Delta_1 \eta t_0) - \frac{\beta \Delta_1 \eta}{\nu e^{-\beta(\Delta_0 - \Delta_1 f_0)}} \ln(1 - \eta) \right). \tag{12}$$

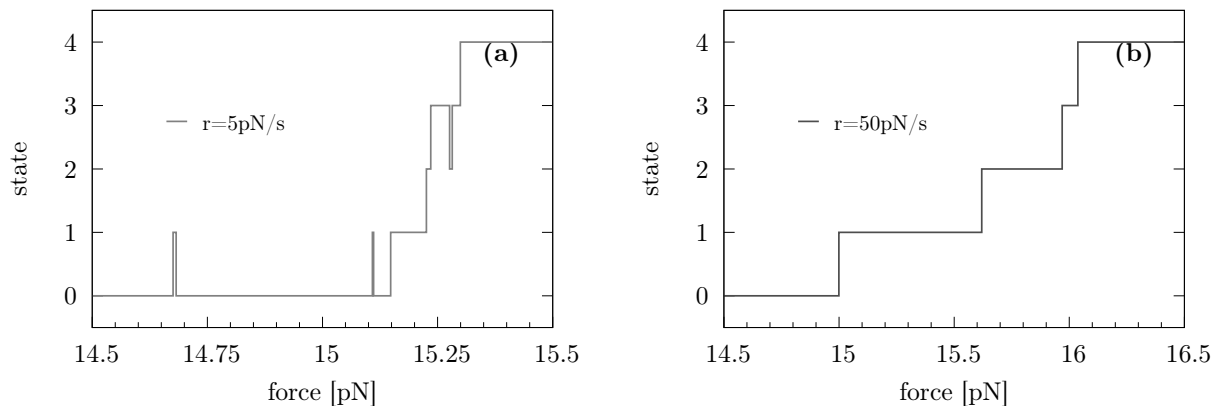


Figure 6. Molecular state as a function of the time-dependent force $f(t) = f_0 + rt$ for two different loading rates r in the relevant time (force) regime of unfolding [for smaller or larger times, the molecule is in the folded ($\alpha = 0$) or unfolded ($\alpha = m$) state, respectively].

Analogously, an attempt time t' for a backward transition is generated from a further random number η' (with Δ'_0 and Δ'_1 replacing Δ_0 and Δ_1). The transition following the previous transition at time t_0 then takes place at time $\min(t, t')$, and the corresponding forward or backward transition is carried out.

In the following we give a detailed presentation of the procedure applied to the sequence III with mixed types of bases in the basic units and interior loops. The other sequences, I and II, are treated in the same way. Let us note that for the sequence I without interior loops, a description of the unfolding kinetics based on a jump dynamics is not really appropriate, because the barriers between minima are too small (see the discussion in section 3.1). Keeping this in mind, we nevertheless include an analysis of this sequence for completeness.

Figure 6 shows typical simulated trajectories for (a) $r = 5$ pN/s and (b) $r = 50$ pN/s, plotted as a function of the time-dependent force $f(t) = f_0 + rt$. As expected from figure 5(a), the first transitions occur at around $f = 15$ pN, and then the molecule rapidly unfolds. Moreover, backward transitions become the less frequent the higher the loading rate r is. In figure 6(a) three backward transitions take place before reaching the unfolded state, while in figure 6(b) no backward transition is seen. If backward transitions are rare before complete unfolding, information on the backward barriers is hardly contained in sampled $\Psi_1(t)$. As a consequence, estimates for Δ'_0 and Δ'_1 will become less accurate for larger r . A good signature for sufficient statistics is that the long-time limit of $\Psi_1(t)$ is between zero and one (see also the discussion further down).

Figure 7(a) shows Ψ_0 sampled from $N = 1000$ trajectories, for three different loading rates. Nonlinear fitting of equation (9) to the data sets with the help of the Levenberg-Marquardt algorithm [57] yields the solid lines.‡ The simulated data follow

‡ In the algorithm, in addition to the estimated $\Psi_j(t)$ values, $j = 0, 1$, their standard deviations $\sigma_j(t)$ need to be given. These can be obtained in the simulations by repeating the procedure for estimating

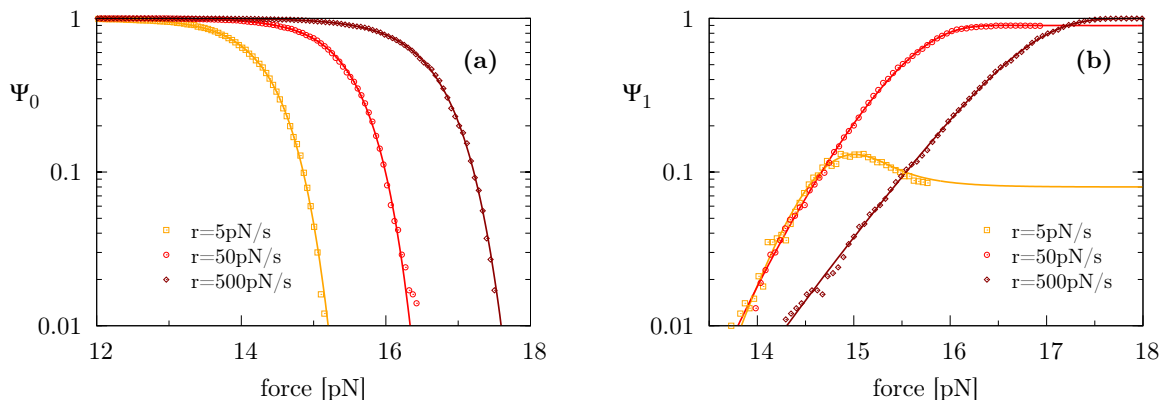


Figure 7. (a) Ψ_0 and (b) Ψ_1 as function of the time-dependent force $f = f(t) = f_0 + rt$. Symbols refer to KMC simulations of $N = 1000$ trajectories for three different loading rates. The solid lines are fits of equations (9) and (10) to the data using the Levenberg-Marquardt algorithm.

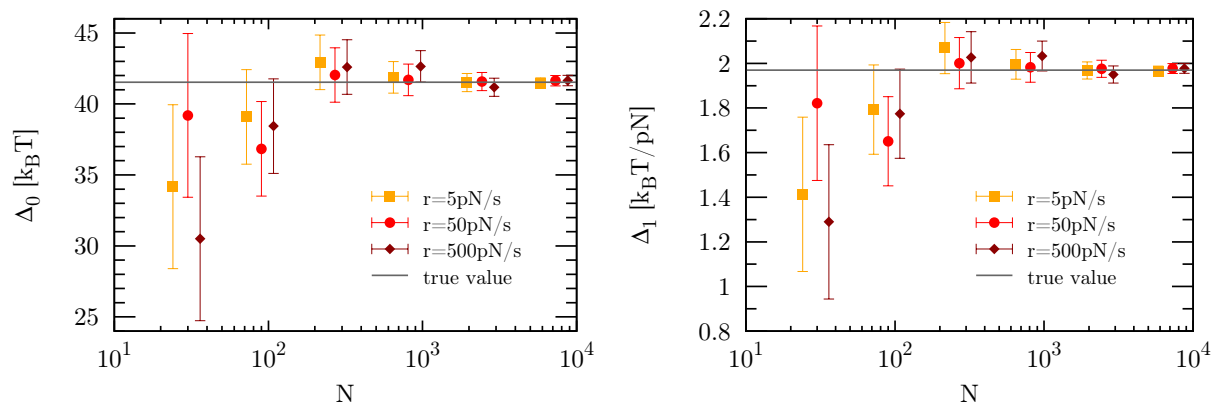


Figure 8. Estimates of Δ_0 (left panel) and Δ_1 (right panel) based on the analysis of N simulated unfolding trajectories for three different loading rates; N values for $r = 5$ pN/s and $r = 500$ pN/s have been slightly shifted for better visibility.

closely the predicted behaviour and the fit parameters are shown in figure 8 as a function of the number of generated trajectories. To obtain 1000 trajectories in single-molecule experiments is already an ambitious task, but not out of reach. Already for about 300 trajectories the fitted Δ_0 and Δ_1 are very close to the true values. In simulations, larger numbers of trajectories can be generated. As is evident from figure 8, the fit parameters converge to the true values for $N \rightarrow \infty$.

With respect to applications, it is encouraging that already for 300 trajectories the fitted Δ_0 and Δ_1 deviate by a few percent only, even when starting the fit at guessed input values which have a deviation of 40 percent from the true parameters. However,

$\Psi_j(t)$ for a large number of sets of N trajectories. They show a pronounced dependence on t , with a maximum in the "unfolding regime" (cf. figure 6). Fortunately, taking time-independent σ_j has a negligible effect on the best fit parameters Δ_j . This means that constant σ_j can be used in an experimental realisation, where only one set of N trajectories is available.

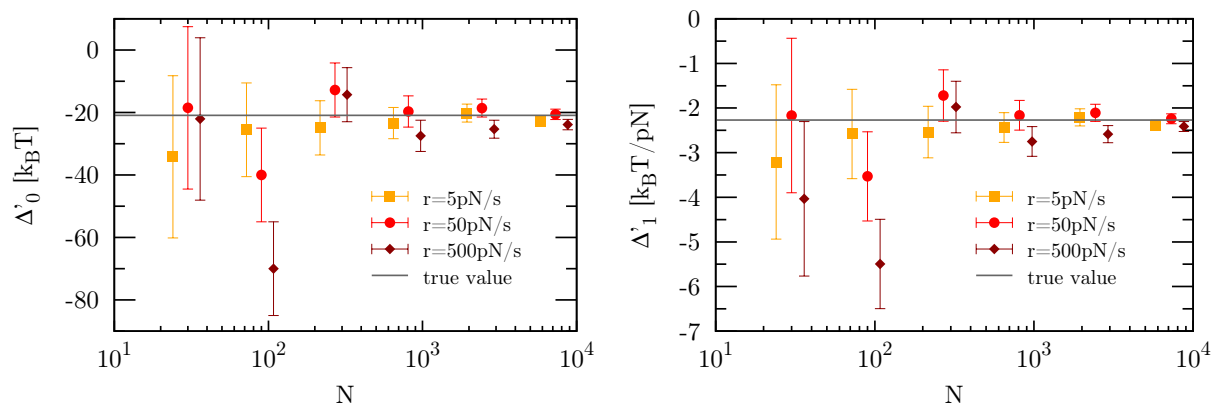


Figure 9. Estimates of Δ'_0 (left panel) and Δ'_1 (right panel) based on the analysis of N simulated unfolding trajectories for three different loading rates; N values for $r = 5$ pN/s and $r = 500$ pN/s have been slightly shifted for better visibility.

in an experiment it would be difficult to estimate the standard deviation. In figure 8 the error bars were obtained by repeating many times the analysis for a given number N of trajectories.

As outlined above, we can now in a second step determine the backward barriers Δ'_0 and Δ'_1 by analysing $\Psi_1(t)$, after fixing the forward barriers to their fitted values. Fits of equation (10) to the KMC data are shown in figure 7(b). The procedure is fully analogous to that of determining Δ_0 and Δ_1 , and figure 9 displays the corresponding results. In fact, with respect to the quality of the fitting, we obtained equivalent findings. In particular, already 300 trajectories are sufficient to yield parameter estimates that deviate by just a few percent from the true values.

Analogous analyses have been performed for the sequences I and II. The corresponding results, as obtained from 1000 trajectories, are listed in the table 2, together with the values from figures 8 and 9 for the sequence III. For the sequence I, it was only possible to extract Δ_0 and Δ_1 , because the backward barriers are so small that backward transitions quickly occur after the first forward transition. As a result, $\Psi_1(t)$ is nearly zero for all t . The same holds true for the sequence II when using the small unfolding rate $r = 5$ pN/s. To overcome this problem, one could generalise the treatment by introducing probabilities that at least $k > 1$ backward transitions occur up to time t . Note that $1 - \psi_1(t)$ is the probability that up to time t at least one backward transition takes place. The complexity of analytical expressions for such probabilities, however, increases with k , which makes a fitting to sampled data difficult in practise. As discussed in section 3.1, application of equilibrium methods would be more suitable for sequences with small energetic barriers. In all cases, where a determination was possible, good estimates of the energetic parameters in equations (4a)-(4c) are obtained. As explained above, the estimates become less accurate at high r , where $\Psi_1(t)$ approaches values close to one at long times. To get good estimates, one can tune the loading rate, such that the long-time limit $\Psi_1(t)$ is about one half.

Table 2. Estimates of the energetic parameters in equations (4a)-(4c) for the sequences I-III based on a sampling of $\Psi_0(t)$ and $\Psi_1(t)$ from $N = 1000$ unfolding trajectories. Results are given for three different loading rates r . An asterisk indicates that a determination of Δ'_0 and Δ'_1 from $\Psi_1(t)$ was not possible (see discussion in main text).

sequence	r	Δ_0	Δ_1	Δ'_0	Δ'_1	g_0	g_1
unit	pN/s	$k_B T$	$\frac{k_B T}{\text{pN}}$	$k_B T$	$\frac{k_B T}{\text{pN}}$	$k_B T$	$\frac{k_B T}{\text{pN}}$
I	true	13.35	0.67	-6.55	-0.45	19.90	1.12
	5	13.34	0.65	*	*	*	*
	50	13.35	0.66	*	*	*	*
	500	13.28	0.64	*	*	*	*
II	true	26.61	1.78	-0.13	-0.79	26.74	2.57
	5	26.63	1.79	*	*	*	*
	50	26.76	1.79	-0.05	-0.78	26.81	2.57
	500	26.59	1.77	0.22	-0.74	26.37	2.51
III	true	41.53	1.97	-20.91	-2.27	62.45	4.23
	5	42.09	2.01	-24.66	-2.51	66.75	4.52
	50	42.41	2.03	-17.43	-2.04	59.84	4.07
	500	39.31	1.83	-15.96	-1.97	55.27	3.80

5. Summary and Conclusions

Based on a commonly used model, we showed that the FEL for different types of DNA hairpin molecules with periodic base sequences is expected to change in a regular manner when applying an external mechanical force f . This regular change manifests itself in forward and backward barriers between successive states that decrease linearly with f over a wide range of forces, covering regimes where molecules completely unfold. Using KMC simulations, stochastic unfolding trajectories were generated as surrogate for experimental ones. With the aim to identify the parameters of the FEL, two probabilities were introduced: The probability $\Psi_0(t)$ that a molecule remains in the folded state until time t , and the probability $\Psi_1(t)$ that until time t , a molecule undergoes at least one forward but no backward transition. These probabilities can be sampled from the trajectories, and theoretical calculations give rather simple expressions for them, allowing one to determine the FEL parameters by a nonlinear fitting procedure. We demonstrated that already about 300 unfolding trajectories are sufficient to obtain good parameter estimates. Best results are obtained if the loading rate is suitably chosen, such that the long-time limit of $\Psi_1(t)$ is neither close to zero nor close to one. For small barriers between states of the order of a few $k_B T$, such rates may become too high to be realisable in experiment.

From a theoretical point of view, the possibility to generate simple functional forms of FELs as function of the number n of open base pairs and applied force f provides an interesting basis for future studies, where exact results could be obtained for kinetic and energetic properties. Analytical results for work distributions will be of particular

interest to gain a deeper understanding of tail regimes.

With respect to applications, our findings provide a promising means to obtain improved values of free energies of interior loops. By attaching loops at regular spacings to homogeneous double strands, periodic sequences can be synthesised and analysed. Taking several periods, good counting statistics should be achieved.

Acknowledgments

Support of this work by the Ministry of Education of the Czech Republic (project no. MSM 0021620835), by the grant agency of the Charles University (grant no. 301311), by the Charles University in Prague (project no. SVV-2013-265 301), and by the Deutsche Akademische Austauschdienst (DAAD, project no. 50755689) is gratefully acknowledged.

Appendix A. Details of the FEL calculation

Taking the sequence 5'-TCCAG...-3' and its complementary part 3'-AGGTC...-5' as an example, the formation energy from equation (2) reads $G_{\text{form}} = \epsilon_{\text{TC}} + \epsilon_{\text{CC}} + \epsilon_{\text{CA}} + \epsilon_{\text{AG}} + \dots$. For its calculation we use the bp energies $\epsilon_{\mu\nu}$ at $T = 25^\circ\text{C}$ and 1 M monovalent salt concentration, as listed in the table A1 [11]. The term G_{loop} in equation (2) refers to the free energy reduction as a result of the release of the end-loop. It is estimated from [39, 50] as $G_{\text{loop}} = 1.58$ kcal/mol.

To account for the elastic response of released ssDNA, different types of models can be assumed to calculate the mean end-to-end distance $u_l(f)$ of the ssDNA in the force direction. The contour length of released ssDNA from n bps is

$$l = 2dn + dn_{\text{loop}}\delta(n, N). \quad (\text{A.1})$$

Here, $d = 0.59$ nm/base [42] is the interphosphate distance and n_{loop} the number of bases per loop. The FJC model, with an extra term suggested in [44], predicts

$$u_l(f) = l \left(1 + \frac{f}{Y} \right) \left[\coth \left(\frac{bf}{k_{\text{B}}T} \right) - \frac{k_{\text{B}}T}{bf} \right], \quad (\text{A.2})$$

Table A1. Nearest-neighbour bp energies (see equation 2) in kcal/mol at $T = 25^\circ\text{C}$ and 1 M monovalent salt concentration [11].

bases	ϵ	bases	ϵ
AA, TT	-1.23	CC, GG	-1.93
AT	-1.17	CG	-2.37
TA	-0.84	GC	-2.36
AC, GT	-1.49	AG, CT	-1.36
CA, TG	-1.66	GA, TC	-1.47

where Y denotes the Young modulus and b the Kuhn length. Under the working conditions for the NN model, one can use $b = 1.15$ nm and $Y = \infty$ [11]. In the WLC model [45], the elastic force for an elongation u_l is

$$f(u_l) = \frac{k_B T}{P} \left[\frac{1}{4(1 - u_l/l)^2} - \frac{1}{4} + \frac{u_l}{l} \right], \quad (\text{A.3})$$

and to obtain $u_l(f)$, this equation has to be inverted; the persistence length P lies in a typical range of 1.0 to 1.5 nm [58].

We have chosen to model $u_l(f)$ according to the FJC model, see equation (A.2). Let us note that both the FJC and WLC approaches give similar good results (for a detailed discussion, see [11, 12]). Because $u_l(f)$ is monotonically increasing with f , it has a unique inverse $f_l(u)$, which is the force exerted by a ssDNA chain with mean end-to-end distance u . Setting $\Delta x_l^{\text{ss}} = u_l(f)$, we obtain

$$G_{\text{str}}^{\text{ss}}(n, f) = \int_0^{\Delta x_l^{\text{ss}}} du' f_l(u') = f \Delta x_l^{\text{ss}} - \int_0^f df' u_l(f'). \quad (\text{A.4})$$

References

- [1] Ritort F 2006 *J. Phys.: Condens. Matter* **18** R531
- [2] Hormeno S and Arias-Gonzalez J R 2006 *Biol. Cell* **98** 679
- [3] Kumar S and Li M 2010 *Phys. Rep.* **486** 1
- [4] Conroy R S and Danilowicz C 2004 *Contemp. Phys.* **45** 277
- [5] Liphardt J, Onoa B, Smith S B, Tinoco I and Bustamante C 2001 *Science* **292** 733
- [6] Collin D, Ritort F, Jarzynski C, Smith S B, Tinoco I and Bustamante C 2005 *Nature* **437** 231
- [7] Greenleaf W J, Woodside M T, Abbondanzieri E A and Block S M 2005 *Phys. Rev. Lett.* **95** 208102
- [8] Woodside M T, Behnke-Parks W M, Larizadeh K, Travers K, Herschlag D and Block S M 2006 *Proc. Natl. Acad. Sci.* **103** 6190
- [9] Mossa A, Manosas M, Forns N, Huguet J M and Ritort F 2009 *J. Stat. Mech.* **P02060**
- [10] Manosas M, Mossa A, Forns N, Huguet J M and Ritort F 2009 *J. Stat. Mech.* **P02061**
- [11] Huguet J M, Bizarro C V, Forns N, Smith S B, Bustamante C and Ritort F 2010 *Proc. Natl. Acad. Sci.* **107** 15431
- [12] Engel S, Alemany A, Forns N, Maass P and Ritort F 2011 *Phil. Mag.* **91** 2049
- [13] Danilowicz C, Coljee V W, Bouzigues C, Lubensky D K, Nelson D R and Prentiss M 2003 *Proc. Natl. Acad. Sci.* **100** 1694
- [14] Janshoff, Neitzert, Oberdörfer and Fuchs 2000 *Angew. Chem.* **39** 3212
- [15] Zhuang X and Rief M 2003 *Curr. Opin. Struct. Biol.* **13** 88
- [16] Alessandrini A and Facci P 2005 *Meas. Sci. Technol.* **16** R65
- [17] Li P T X, Collin D, Smith S B, Bustamante C and Tinoco I 2006 *Biophys. J.* **90** 250
- [18] Alemany A, Mossa A, Junier I and Ritort F 2012 *Nat. Phys.* **8** 688
- [19] Ribezzi-Crivellari M, Huguet J M and Ritort F 2013 *Rev. Sci. Instrum.* **84** 043104
- [20] Cocco S, Marko J F and Monasson R 2003 *Eur. Phys. J. E* **10** 153
- [21] Esposito M and Van den Broeck C 2010 *Phys. Rev. Lett.* **104** 090601
- [22] Seifert U 2012 *Rep. Prog. Phys.* **75** 126001
- [23] Crooks G E 1999 *Phys. Rev. E* **60** 2721
- [24] Jarzynski C 1997 *Phys. Rev. Lett.* **78** 2690
- [25] Hummer G and Szabo A 2001 *Proc. Natl. Acad. Sci.* **98** 3658
- [26] Harris N C, Song Y and Kiang C H 2007 *Phys. Rev. Lett.* **99** 068101

- [27] Liphardt J, Dumont S, Smith S B, Tinoco I and Bustamante C 2002 *Science* **296** 1832
- [28] Ritort F, Bustamante C and Tinoco I 2002 *Proc. Natl. Acad. Sci.* **99** 13544
- [29] Zuckerman D M and Woolf T B 2002 *Phys. Rev. Lett.* **89** 180602
- [30] Gore J, Ritort F and Bustamante C 2003 *Proc. Natl. Acad. Sci.* **100** 12564
- [31] Engel A 2009 *Phys. Rev. E* **80** 021120
- [32] Nickelsen D and Engel A 2011 *Eur. Phys. J. B* **82** 207
- [33] Palassini M and Ritort F 2011 *Phys. Rev. Lett.* **107** 060601
- [34] Wood R H, Muehlbauer W C F and Thompson P T 1991 *J. Phys. Chem.* **95** 6670
- [35] Fox R F 2003 *Proc. Natl. Acad. Sci.* **100** 12537
- [36] Shirts M R, Bair E, Hooker G and Pande V S 2003 *Phys. Rev. Lett.* **91** 140601
- [37] Ritort F 2008 *Adv. Chem. Phys.* **137** 31
- [38] Manosas M, Collin D and Ritort F 2006 *Phys. Rev. Lett.* **96** 218301
- [39] SantaLucia J J 1998 *Proc. Natl. Acad. Sci.* **95** 1460
- [40] Lubensky D K and Nelson D R 2002 *Phys. Rev. E* **65** 031917
- [41] Manosas M and Ritort F 2005 *Biophys. J.* **88** 3224
- [42] Huguet J M, Forns N and Ritort F 2009 *Phys. Rev. Lett.* **103** 248106
- [43] de Messieres M, Brawn-Cinani B and La Porta A 2011 *Biophys. J.* **100** 2736
- [44] Smith S B, Cui Y and Bustamante C 1996 *Science* **271** 795
- [45] Bustamante C, Marko J F, Siggia E D and Smith S 1994 *Science* **265** 1599
- [46] Crothers D M and Zimm B H 1964 *J. Mol. Biol.* **9** 1
- [47] Devoe H and Tinoco I J 1962 *J. Mol. Biol.* **4** 500
- [48] Talukder S, Chaudhury P, Metzler R and Banik S K 2011 *J. Chem. Phys.* **135** 165103
- [49] Gross P, Laurens N, Oddershede L B, Bockelmann U, Peterman E J G and Lwuite G J 2011 *Nat. Phys.* **7** 731
- [50] Zuker M 2003 *Nucleic Acids Res.* **31** 3406
- [51] Bell G I 1978 *Science* **200** 618
- [52] Brey and Prados 1991 *Phys. Rev. B* **43** 8350
- [53] Šubr E and Chvosta P 2007 *J. Stat. Mech.* **2007** P09019
- [54] Holubec V, Chvosta P and Maass P 2012 *J. Stat. Mech.* **P11009**
- [55] Einax M and Maass P 2009 *Phys. Rev. E* **80** 020101
- [56] Holubec V, Chvosta P, Einax M and Maass P 2011 *Europhy. Lett.* **93** 40003
- [57] Press W H, Teukolsky S A, Vetterling W T and Flannery B P 1997 *Numerical recipes in Fortran 90* 2nd ed vol 2 (Cambridge University Press)
- [58] Dessinges M N, Maier B, Zhang Y, Peliti M, Bensimon D and Croquette V 2002 *Phys. Rev. Lett.* **89** 248102